Supplementary Material

Supplementary Case Study

1. Case Study of Yecheon

1.1. Study Area and Data Acquisition

One more case site, the Pori-cheon stream in Yecheon-gun was selected to reveal the performance of the proposed KLR model with the point cloud as shown in Figure 18. Four sites were ground-surveyed with the EMLID Reach RS2 and aerial surveying was also performed with the Autel Evo II. For this site, the same UAV and GPS tool were used as the REC in section 4. The Y1 is located in the upper stream of the Pori-cheon stream than the Y4. The cross-section of Y2 is located in the right below of the bridge followed by the Y3 cross-section. The detailed shape of the cross-section is shown from Figure 19 and Figure 20 for each cross-section. At each section, 10-12 points were ground-surveyed and the point cloud were abstracted with Pix4D mapper while the bottom width is about 10m. The demarcation of the cross-section with the tested KLR, LOWESS, and Polyfit models was performed.

1.2. Results

The shape of the Y1 cross-section presents the rough river bottom (the left panels of Figure 19) while the left section has lower bottom and the section should be major flow passage during low streamflow. The other side of this cross-section has further ups and downs possibly by debris and riparian vegetation. These ups and downs were not measured in detail by ground surveying. Additional ground surveying can capture the characteristic. However, it requires further time consumption for measurement and the accessibility cannot be guaranteed even in such a small stream. Meanwhile, the point cloud captures the detailed characteristics of the channel bottom and KLR model describes the characteristics as shown in the panel(a-1) of Figure 19 following the major cloud data. In LOWESS, the Y1 cross-section is not presented with missing the abrupt change in both walls of the cross-section (the panel(b-1) of Figure 19)

and all the Polyfit models (see the pane(c-1)) present similar behavior as the result of the LOWSS. The wall part (5-6m and 17-18m of the cross-section) was not well reproduced by the Polyfit models. The RMSE and MAE in Table S2 present the superiority of the KLR for the Y1 cross-section. The RMSE and MAE of the Y1 is rather larger than the other cross-section. This large error might be induced from the ups and downs of the channel bottom.

Meantime, the Y2 cross-section in the right panels of Figure 19 shows similar to the U-shape of a natural river in Figure 6. The ground-surveyed points (blue solid line with cross markers in the right panels of Figure 19) are matched well with the point cloud data except the slight deviation at the left-top embankment (in 2-3m). This U-shape cross-section is demarcated well with the KLR model while slight underestimation can be observed with the LOWESS model in the right embankment (13-14m). Not much good performance can be seen with all the Polyfit models shown at the panel(c-2) of Figure 19. The RMSE and MAE in Table S2. also show the worst performance in the Polyfit models and superiority with the KLR model.

The Y3 and Y4 cross-sections in Figure 20, respectively, present traditional man-made trapezoid shape. These trapezoid channels were modeled both with KLR and LOWESS while the KLR presents better descriptive characteristics in the abrupt changing part of the cross-section. While the Polyfit-4 presents fair performance to model the Y4 cross-section in the right panels of Figure 20, the Y3 was not demarcated well with all the Polyfit models (see the panel(c-2)). The RMSE of the KLR model is only 0.092 and 0.068 while the LOWESS shows 0.236 and 0.116 for the Y3 and Y4 cross-sections in Table S2. The results indicate that the KLR model presents superiority among all the tested LOWESS and Polyfit models in case of all different shapes as the irregular U-shape, trapezoid-shape channels in the Pori-cheon stream, Yecheon.

Equations

Polynomial Regression

A polynomial regression model can be used when the relationship between a predictor (x) and an explanatory variable (y) is nonlinear or curvilinear. The Mth-order polynomial regression can be expressed as

$$y = \beta_0 + \beta_1 x + \beta_2 x^2 + \cdots + \beta_k x^M + \epsilon = \sum_{i=0}^{M} \beta_i x^i + \epsilon = \mathbf{x\beta} + \epsilon \quad \text{(S1)}$$

where ϵ is considered to be a random noise with zero mean and M is the degree of the polynomial regression model, called PolyFit. Here, x can be the distance from the base location in a river cross-section with a length unit (meter, in the current study) and y is the elevation with the same length unit (meter as well).

According to its degree M, the model is structured as follows.

$$y = \beta_0 + \beta_1 x + \beta_2 x^2 + \epsilon \quad \text{(S2)}$$

$$y = \beta_0 + \beta_1 x + \beta_2 x^2 + \beta_3 x^3 + \epsilon \quad \text{(S3)}$$

$$y = \beta_0 + \beta_1 x + \beta_2 x^2 + \beta_3 x^3 + \beta_4 x^4 + \epsilon \quad \text{(S4)}$$

Eq. (2), Eq. (3), and Eq. (4) in the manuscript are defined as PolyFit2, PolyFit3, and PolyFit4, respectively, and employed in the current study.

LOcally WEighted Scatterplot Smoothing (LOWESS)

The LOWESS with one explanatory variable (x_t, the distance from the base location for x-coordinate) and one predictor variable (y_t, the elevation of the corresponding tth point) can be defined as

$$y_t = m(x_t) + \varepsilon_t \quad \text{(S5)}$$

where the regression curve m($\mathbf{y}_t$) is the conditional expectation $m(x_t) = E(Y|X = x_t)$. The LOWESS estimate can be defined as

$$\widehat{m}_{LOWESS}(x_t) = \vec{x}_t^T \widehat{\boldsymbol{\beta}}_t^{LOWESS} \quad \text{(S6)}$$

where

$$\widehat{\boldsymbol{\beta}}_t^{LOWESS} = (\vec{\mathbf{X}}_t{}^T \boldsymbol{W}_t \vec{\mathbf{X}}_t)^{-1} \vec{\mathbf{X}}_t{}^T \boldsymbol{W}_t \mathbf{y} \quad \text{(S7)}$$

with $\vec{\mathbf{X}}_t$as the difference matrix between the current condition and observed data and $\boldsymbol{W}_t$is the kernel weights with a bandwidth matrix.

Tables

Table S1. Information for the tested four sites in the engineering study of 2019.

	X	Z		X	Z

Site-1	1	0	18.18	Site-3	1	0	18.32
	2	4.4	18.18		2	3.12	19.75
	3	7.48	19.76		3	5.8	19.75
	4	10.98	19.8		4	6.1	19.47
	5	12.24	19.38		5	7.1	19.47
	6	13.5	19.38		6	12.62	15.8
	7	19.5	15.47		7	24.4	15.25
	8	23.82	15.81		8	30.7	15.67
	9	28.08	16.68		9	36.2	19.48
	10	32.28	19.42		10	37.76	19.48
	11	33.66	19.42		11	38.82	19.9
	12	34.92	19.9		12	41.86	19.9
	13	37.92	19.9		13	45.02	18.54
					14	46.82	18.54
		X	Z			X	Z
Site-2	1	0	17.46	Site-4	1	0	17.64
	2	9.06	17.82		2	2.6	17.64
	3	10.26	19.68		3	5.54	19.68
	4	13.48	19.68		4	8.94	19.68
	5	14.42	19.39		5	11.14	19.48
	6	15.42	19.39		6	15.7	16.53
	7	21.76	15.04		7	19.42	16.53
	8	26.24	14.7		8	20.92	16.08
	9	30.32	14.98		9	23.18	16.52
	10	37	19.36		10	24.54	16.52
	11	38.5	19.36		11	26.6	15.75
	12	39.8	19.89		12	29.08	15.98
	13	43	19.89		13	37	19.83
	14	46.32	18.35		14	40	19.83
	15	47.94	18.35				

Table S2. Performance measures of MAE and RMSE for three different models as KLR, LOWESS, and PolyFit for Yecheon.

	Site No.	KLR	LOWESS	PolyFit2	PolyFit3	PolyFit4
RMSE	Y1	**0.235**	0.461	0.652	0.566	0.533
	Y2	**0.135**	0.279	0.750	0.721	0.377
	Y3	**0.092**	0.236	0.693	0.659	0.401
	Y4	**0.068**	0.116	0.425	0.362	0.124

MAE	Y1	**0.158**	0.356	0.544	0.446	0.435
	Y2	**0.098**	0.223	0.678	0.647	0.289
	Y3	**0.073**	0.178	0.634	0.571	0.353
	Y4	**0.047**	0.079	0.240	0.232	0.108

Figures

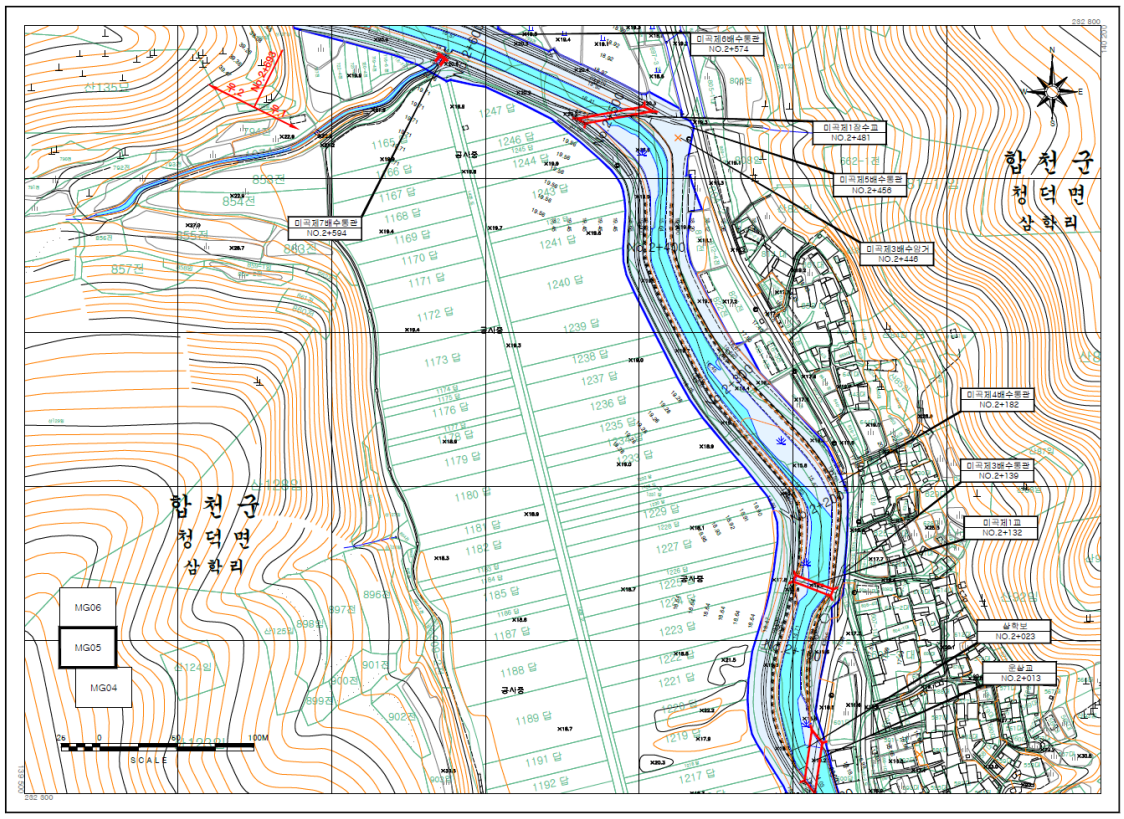

Figure S1. Plane map of the study area from the engineered study of 2019 (Migok-cheon stream).

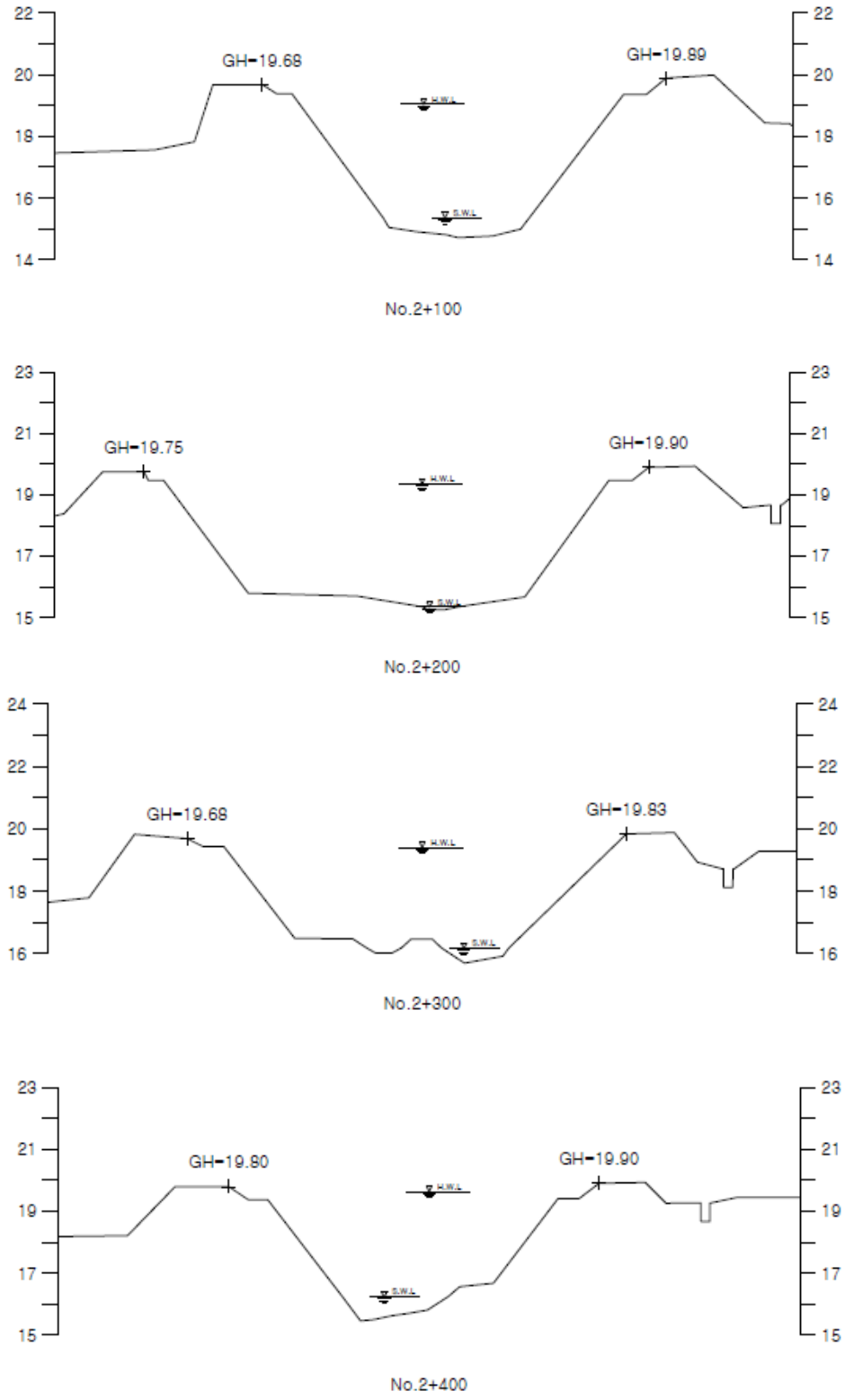

Figure S2. Cross-sections of the tested site of the study area from the engineered study of 2019 (Migok-cheon stream).

Figure S3. Pictures of (a) EMILID Reach RS2 for ground surveying and (b) its installed system; and (c) the employed UAV of the EVO II and (d) its controller.

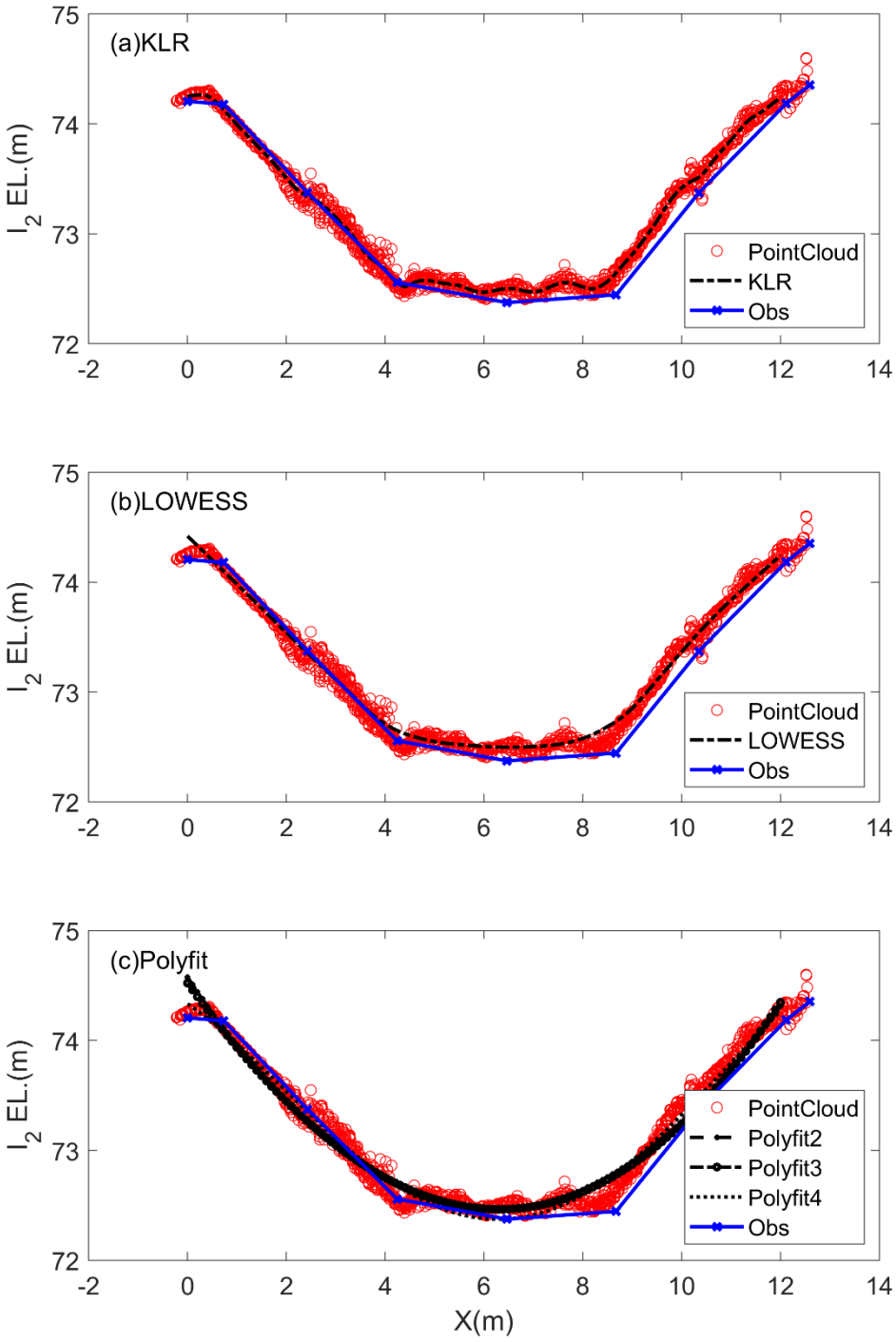

Figure S4. Point cloud data (red circles) for the channel I_2 of the REC and model-fitted line (black dashed line) with KLR (panel(a)), LOWESS (panel(b)), and PolyFit (panel(c)) as well as the ground surveying (blue solid line with x marker).

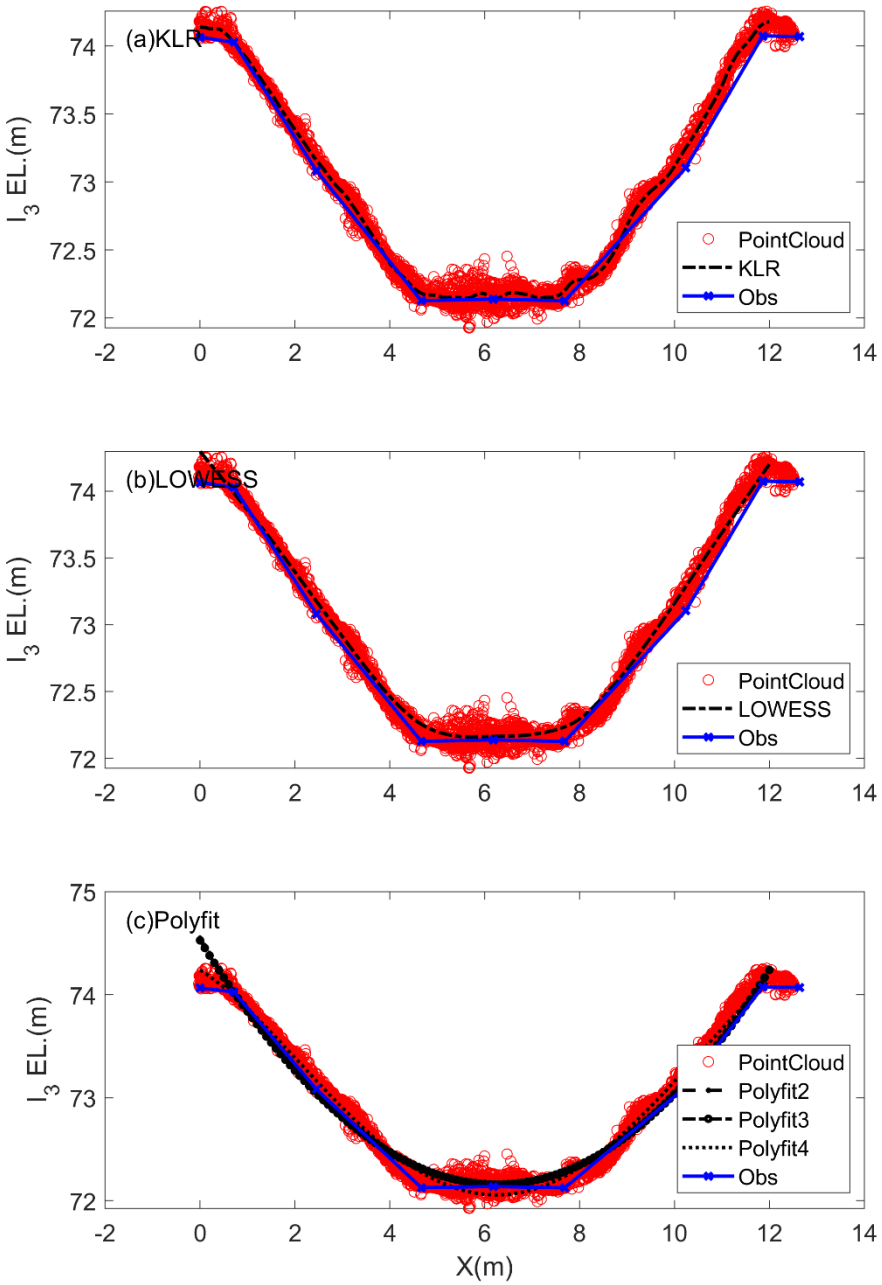

Figure S5. Point cloud data (red circles) for the channel I_3 of the REC and model-fitted line (black dashed line) with KLR (panel(a)), LOWESS (panel(b)), and PolyFit (panel(c)) as well as the ground surveying (blue solid line with x marker).

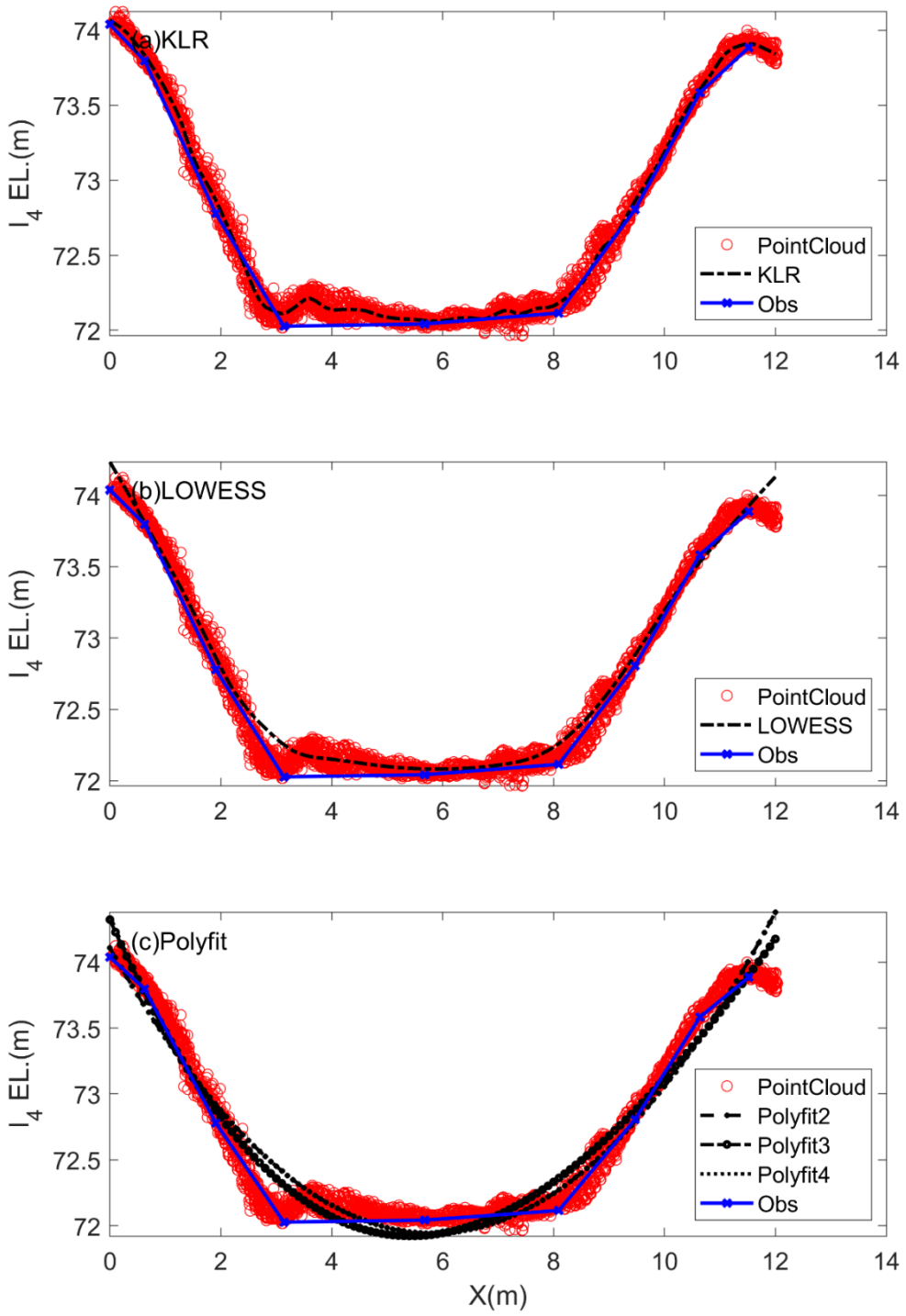

Figure S6. Point cloud data (red circles) for the channel I_4 of the REC and model-fitted line (black dashed line) with KLR (panel(a)), LOWESS (panel(b)), and PolyFit (panel(c)) as well as the ground surveying (blue solid line with x marker).

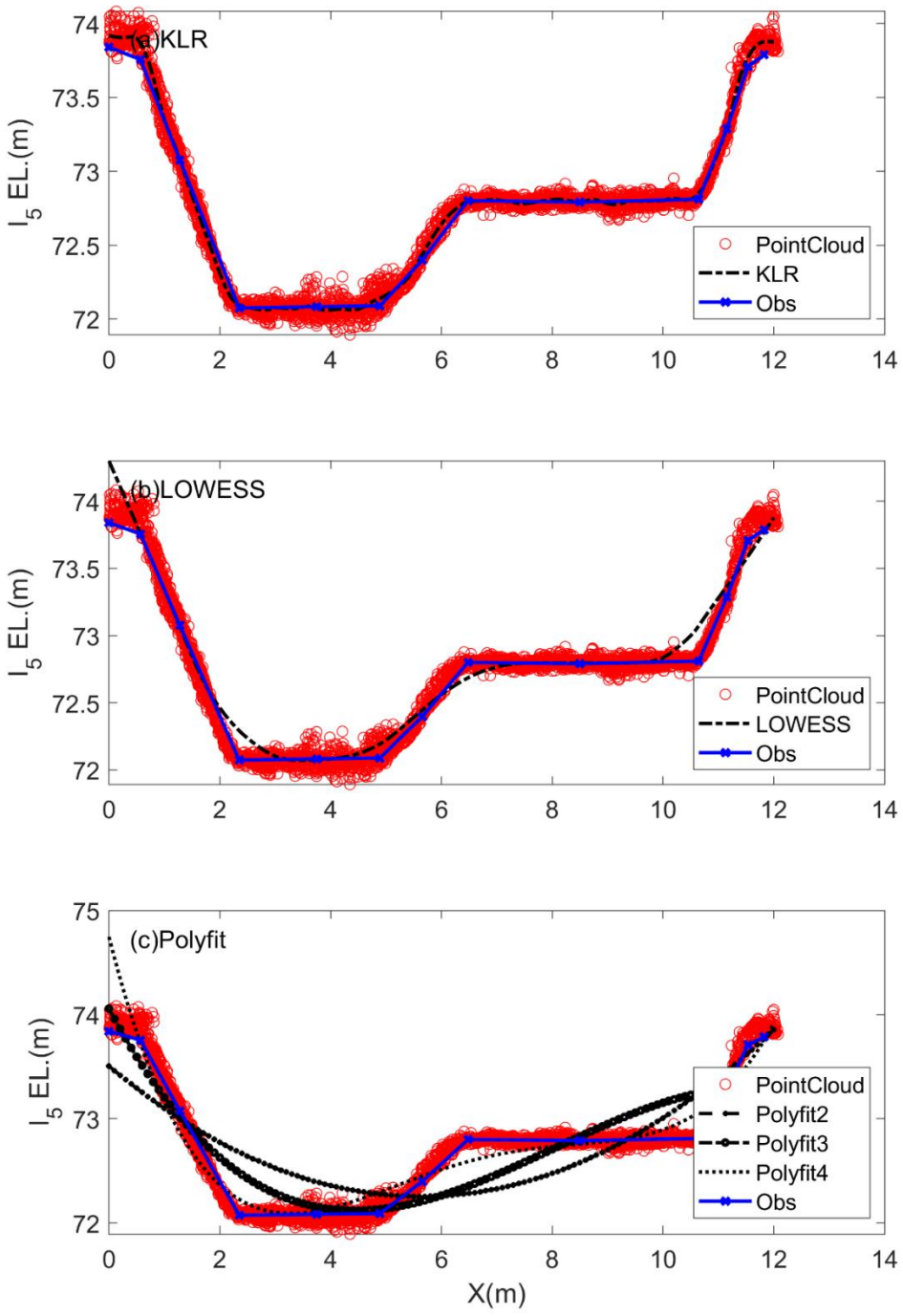

Figure S7. Point cloud data (red circles) for the channel I_5 of the REC and model-fitted line (black dashed line) with KLR (panel(a)), LOWESS (panel(b)), and PolyFit (panel(c)) as well as the ground surveying (blue solid line with x marker).

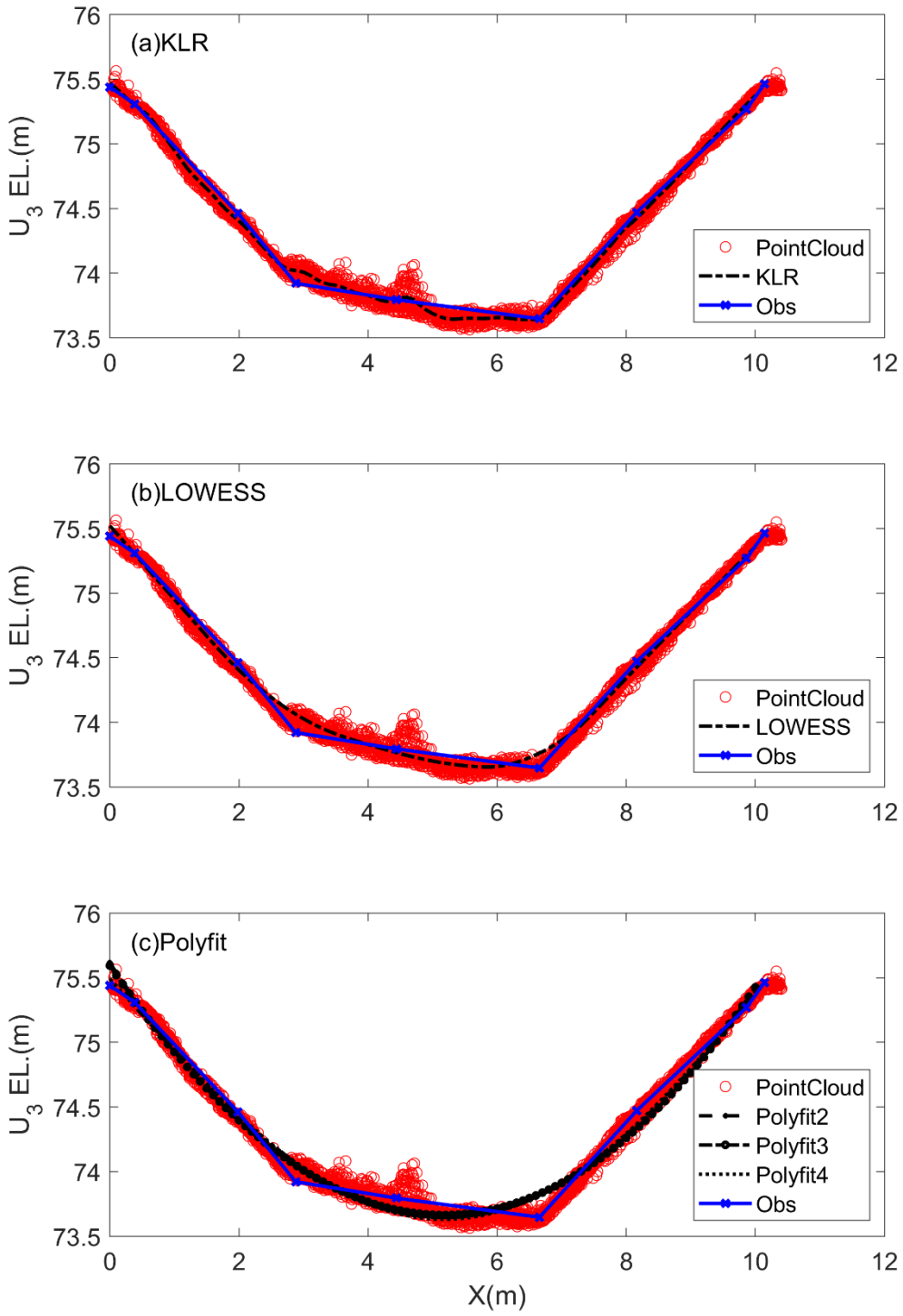

Figure S8. Point cloud data (red circles) for the channel U_3 of the REC and model-fitted line (black dashed line) with KLR (panel(a)), LOWESS (panel(b)), and PolyFit (panel(c)) as well as the ground surveying (blue solid line with x marker).

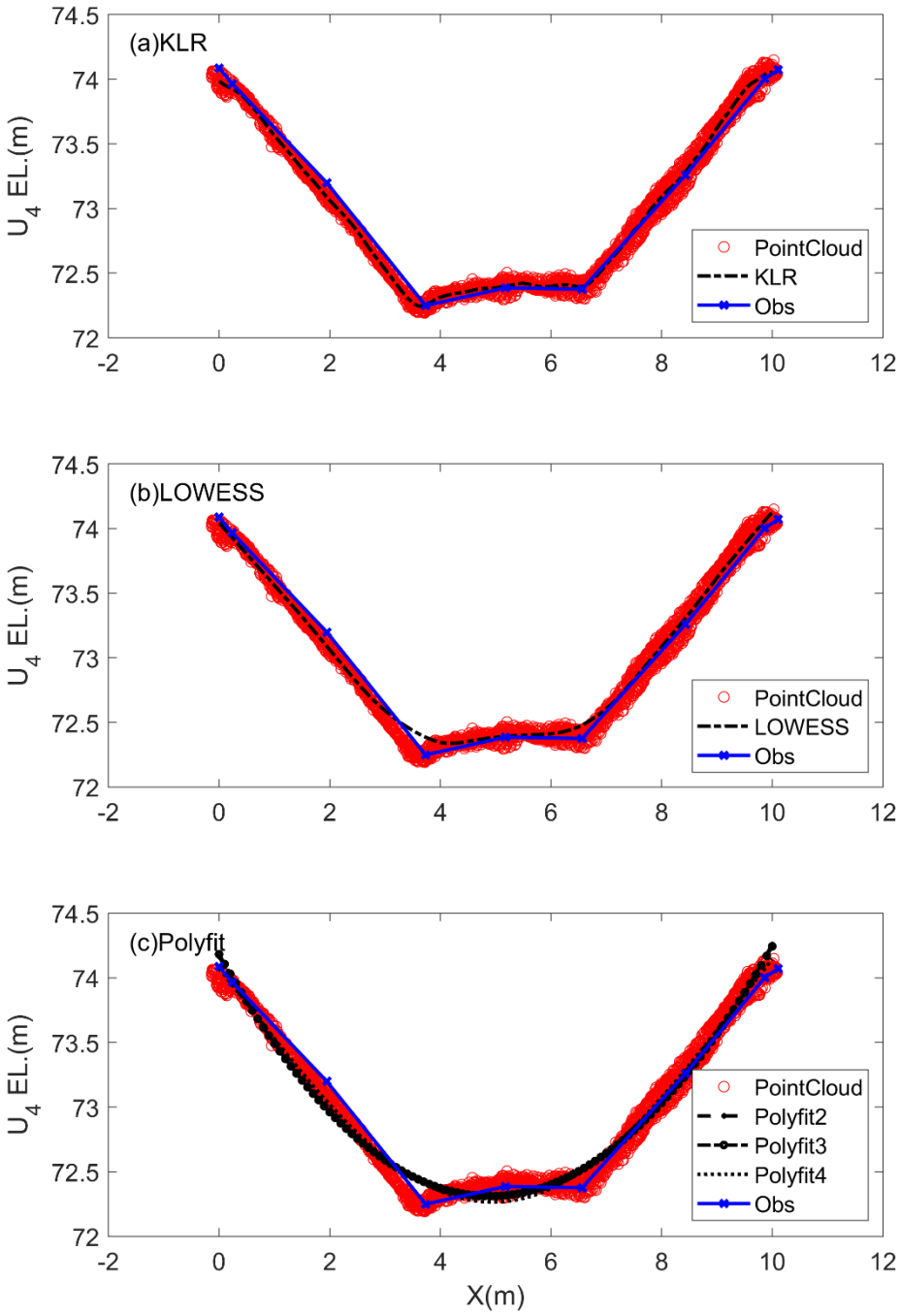

Figure S9. Point cloud data (red circles) for the channel U_4 of the REC and model-fitted line (black dashed line) with KLR (panel(a)), LOWESS (panel(b)), and PolyFit (panel(c)) as well as the ground surveying (blue solid line with x marker).

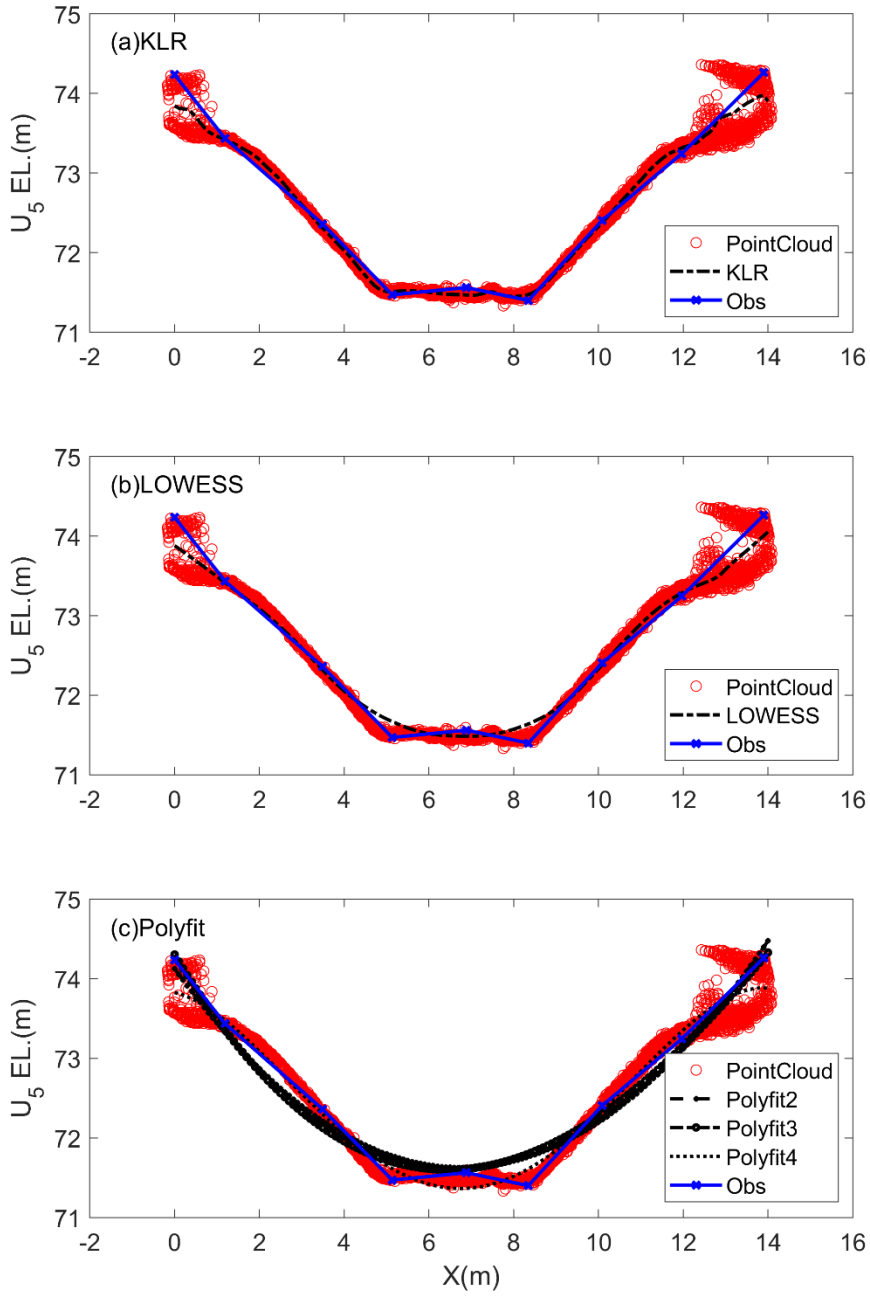

Figure S10. Point cloud data (red circles) for the channel U_5 of the REC and model-fitted line (black dashed line) with KLR (panel(a)), LOWESS (panel(b)), and PolyFit (panel(c)) as well as the ground surveying (blue solid line with x marker).

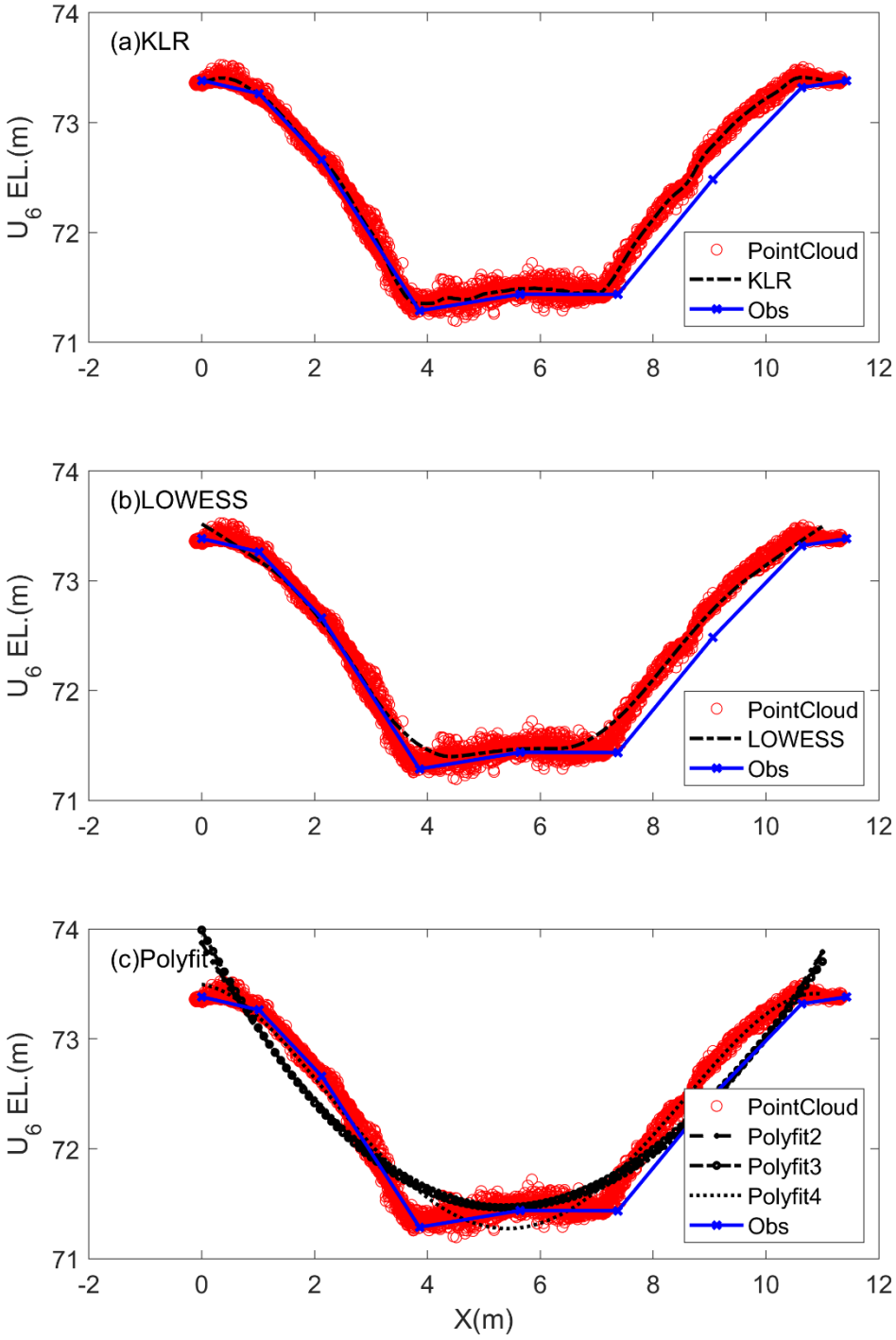

Figure S11. Point cloud data (red circles) for the channel U_6 of the REC and model-fitted line (black dashed line) with KLR (panel(a)), LOWESS (panel(b)), and PolyFit (panel(c)) as well as the ground surveying (blue solid line with x marker).

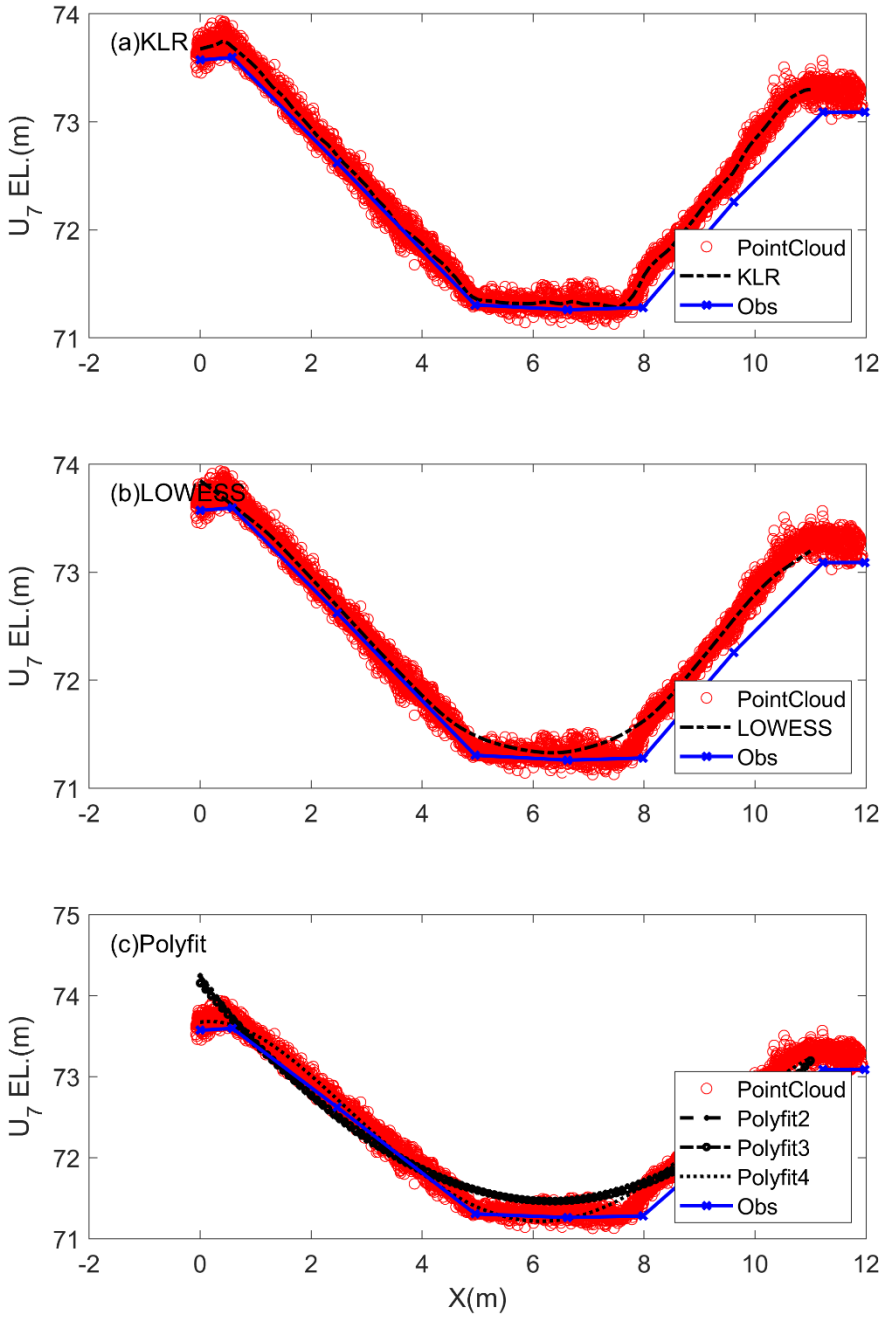

Figure S12. Point cloud data (red circles) for the channel U_7 of the REC and model-fitted line (black dashed line) with KLR (panel(a)), LOWESS (panel(b)), and PolyFit (panel(c)) as well as the ground surveying (blue solid line with x marker).

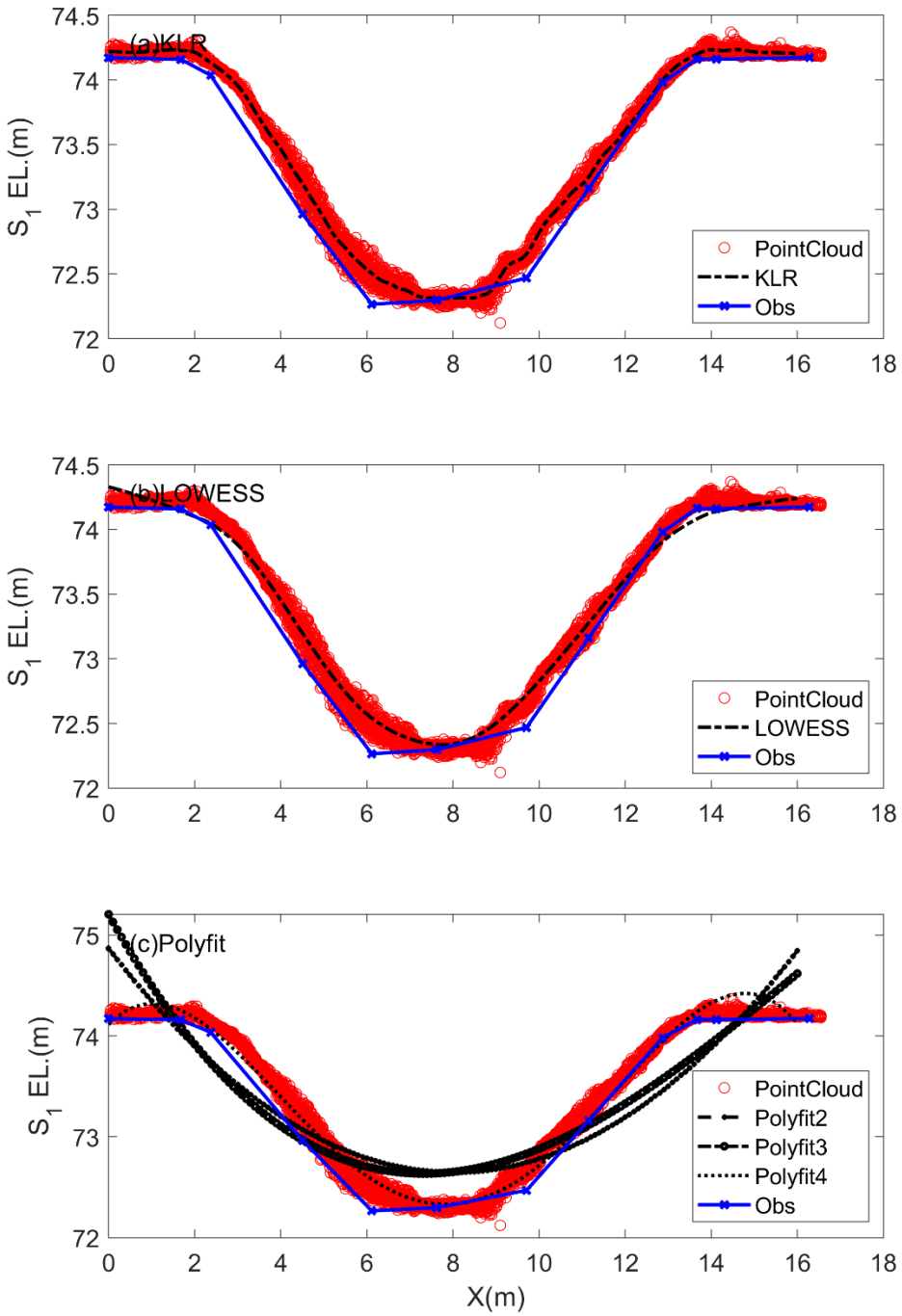

Figure S13. Point cloud data (red circles) for the channel S_1 of the REC and model-fitted line (black dashed line) with KLR (panel(a)), LOWESS (panel(b)), and PolyFit (panel(c)) as well as the ground surveying (blue solid line with x marker).

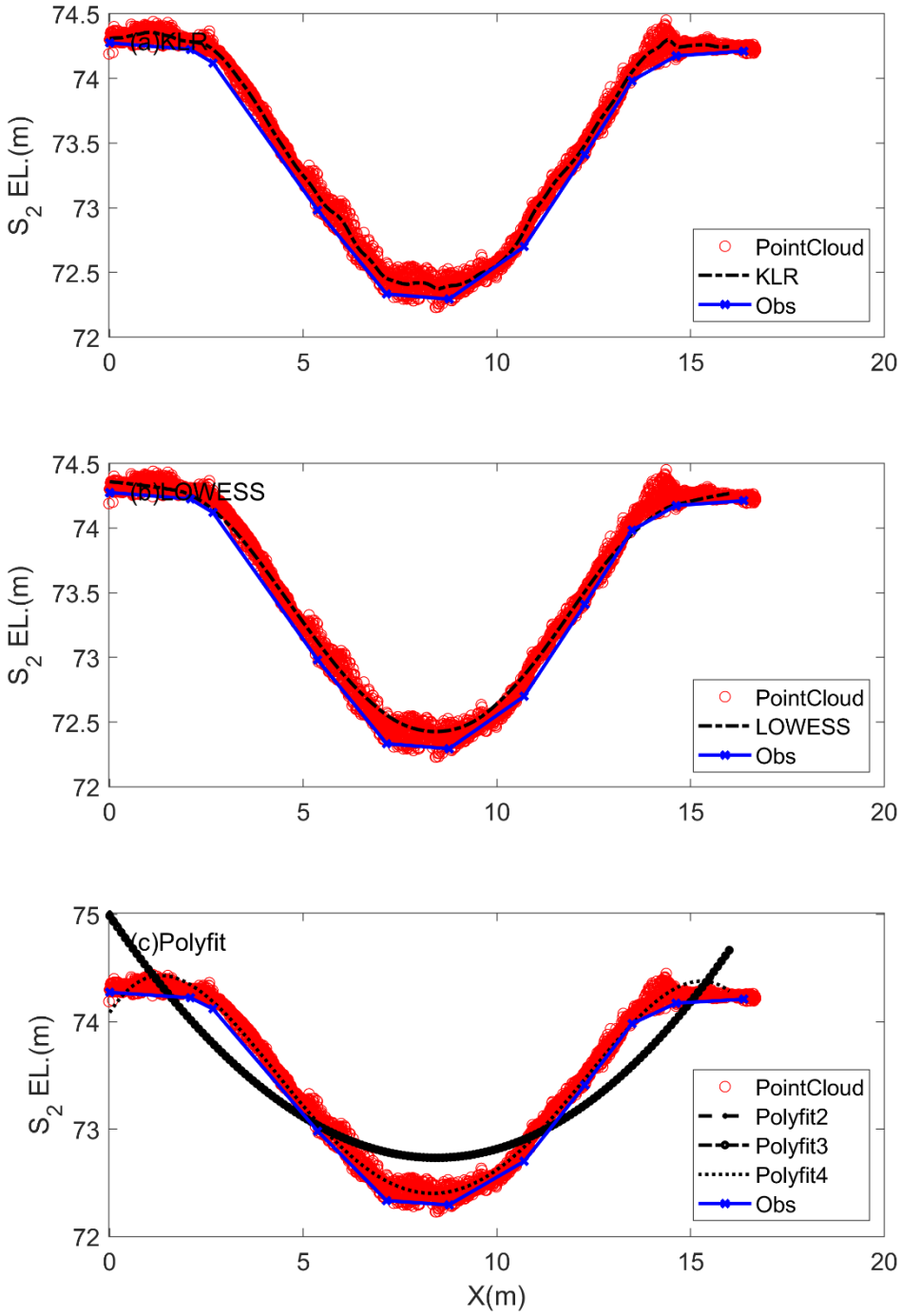

Figure S14. Point cloud data (red circles) for the channel S_2 of the REC and model-fitted line (black dashed line) with KLR (panel(a)), LOWESS (panel(b)), and PolyFit (panel(c)) as well as the ground surveying (blue solid line with x marker).

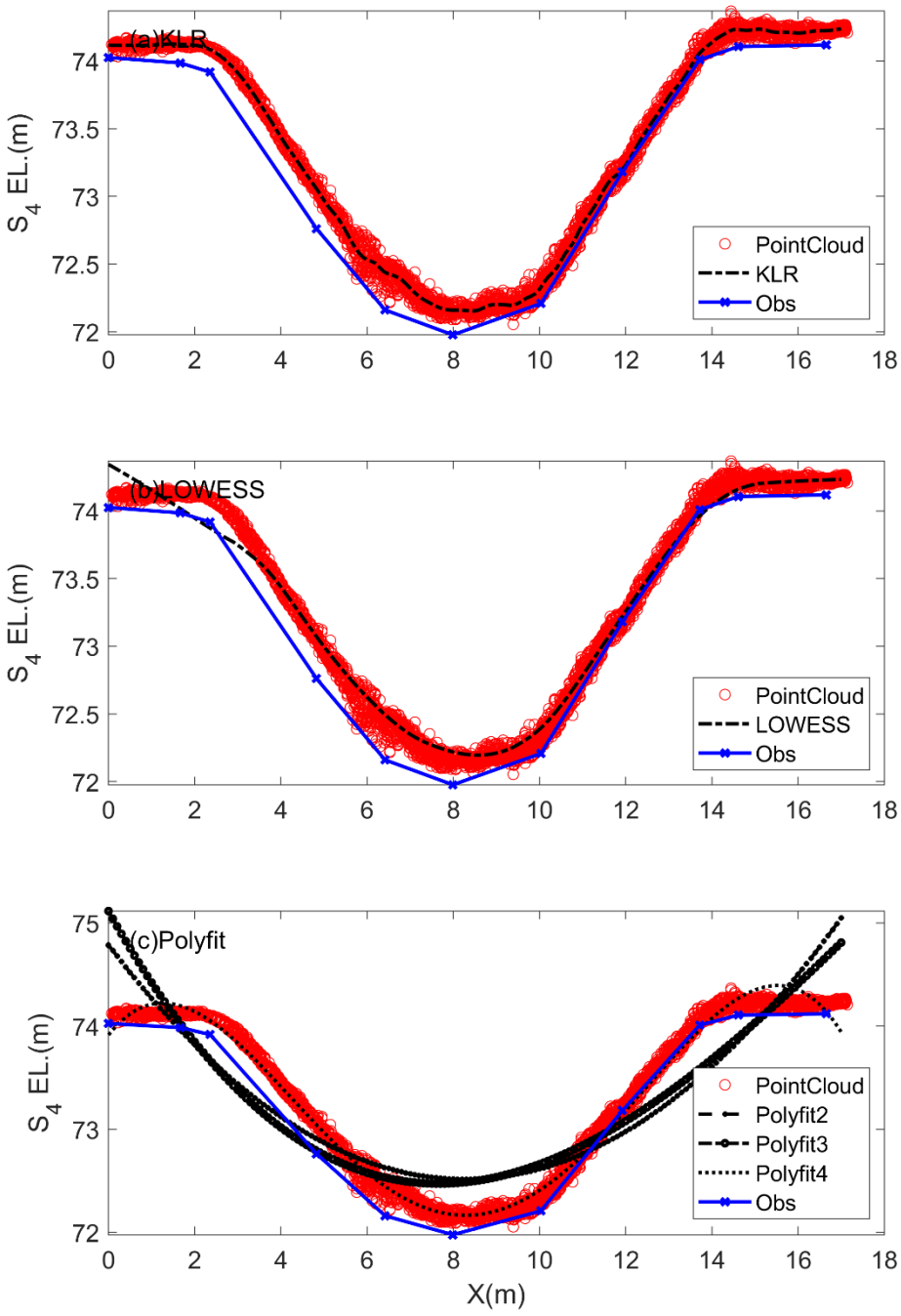

Figure S15. Point cloud data (red circles) for the channel S_4 of the REC and model-fitted line (black dashed line) with KLR (panel(a)), LOWESS (panel(b)), and PolyFit (panel(c)) as well as the ground surveying (blue solid line with x marker).

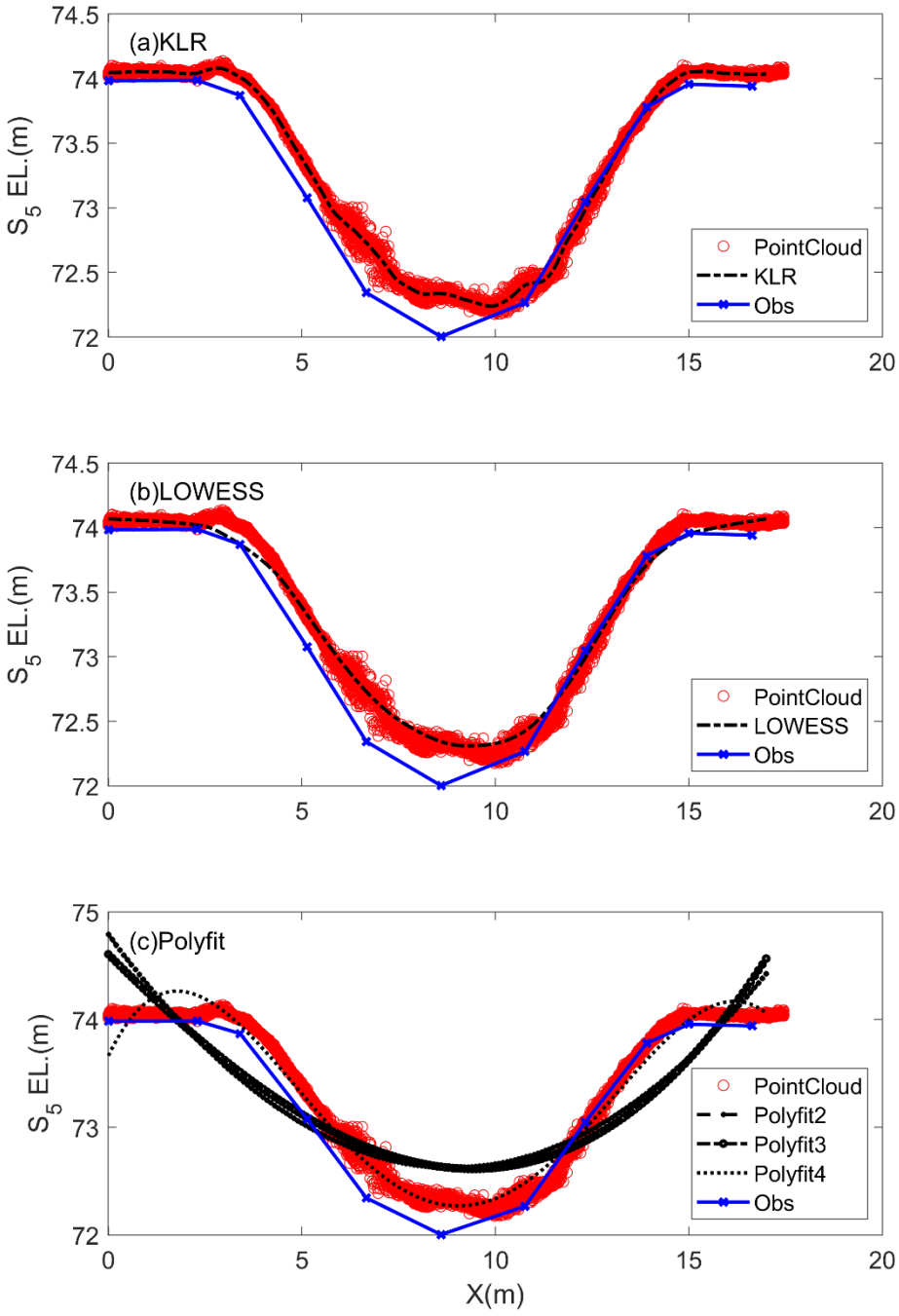

Figure S16. Point cloud data (red circles) for the channel S_5 of the REC and model-fitted line (black dashed line) with KLR (panel(a)), LOWESS (panel(b)), and PolyFit (panel(c)) as well as the ground surveying (blue solid line with x marker).

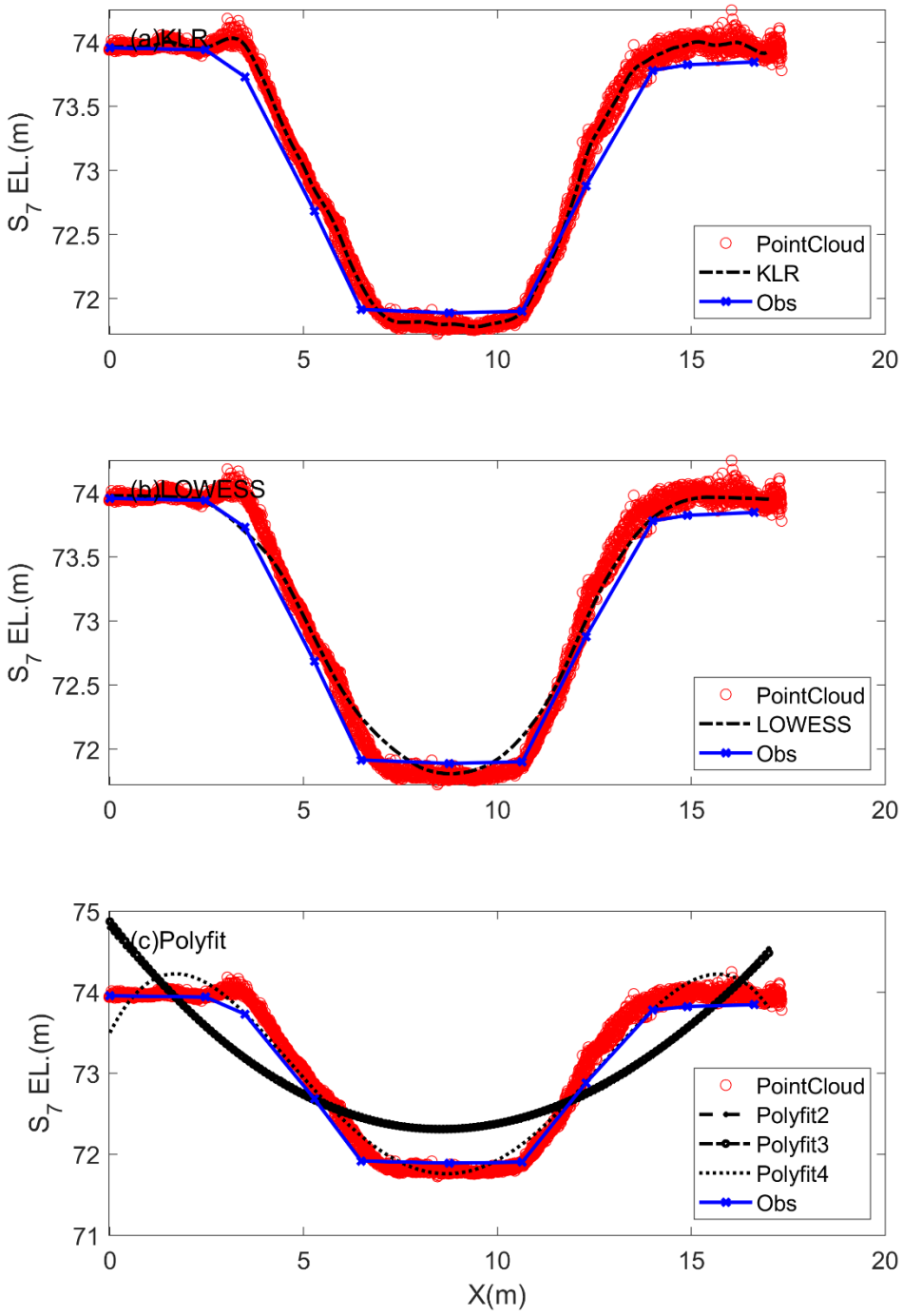

Figure S17. Point cloud data (red circles) for the channel S_7 of the REC and model-fitted line (black dashed line) with KLR (panel(a)), LOWESS (panel(b)), and PolyFit (panel(c)) as well as the ground surveying (blue solid line with x marker).

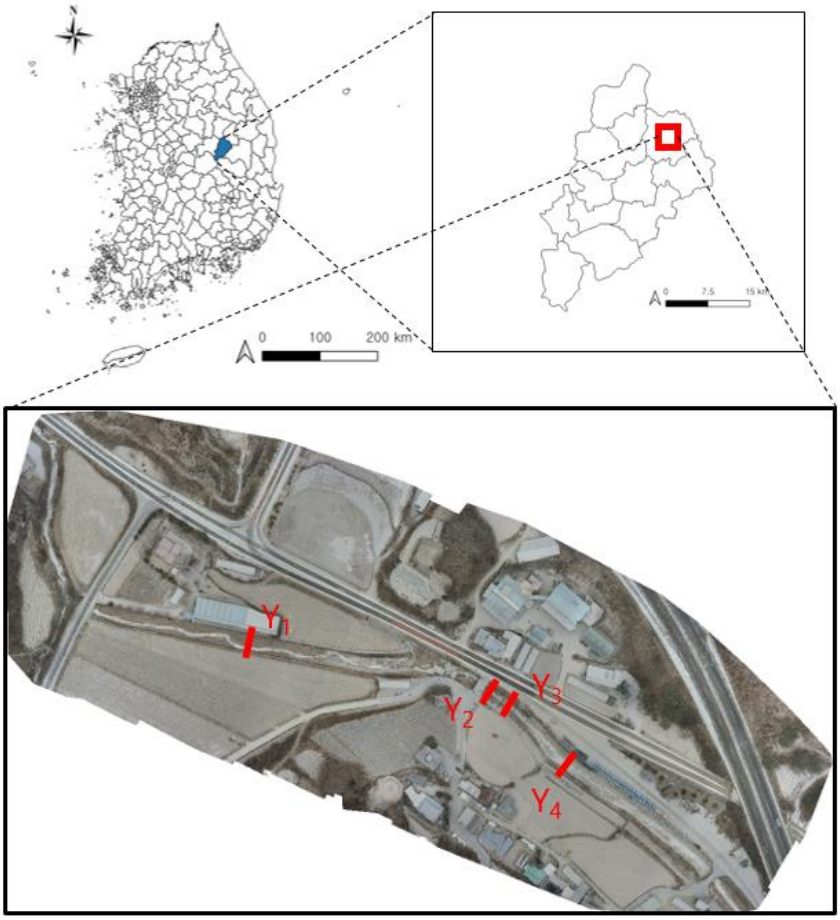

Figure 18. Study area of the applied stream, Pori-cheon stream in Yecheon-gun (Blue area in the top left panel) South Korea. The aerial image is taken and produced by the authors and no copyright is required.

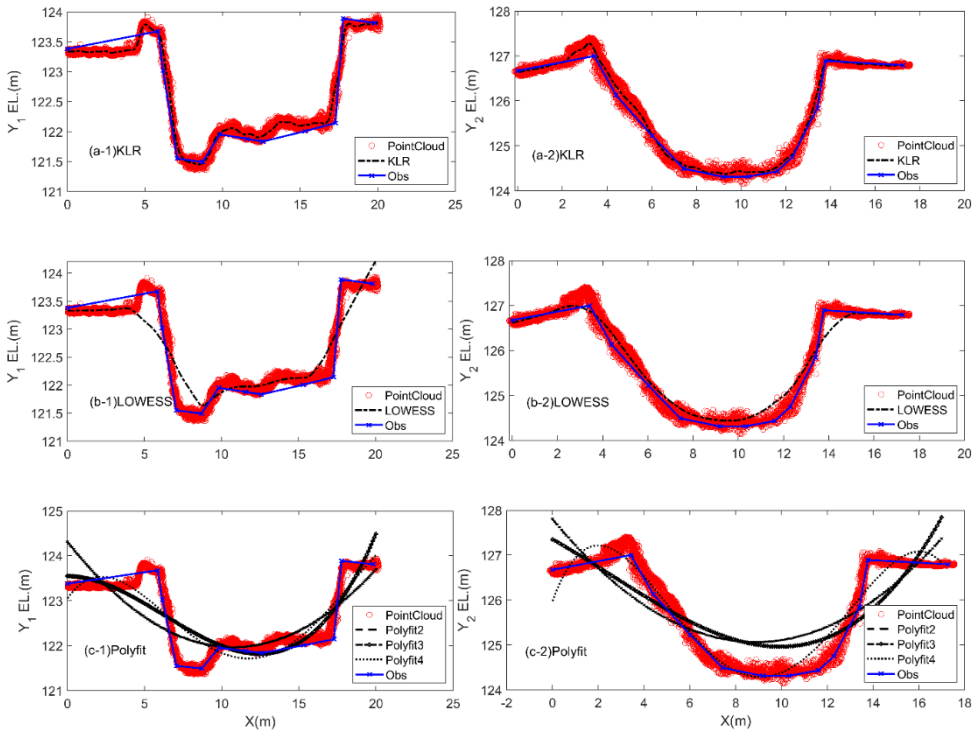

Figure 19. Point cloud data (red circles) for the Y_1 (left panels) and Y_2 (right panels) of Yecheon site and model-fitted line (black dashed line) with KLR (panel(a)), LOWESS (panel(b)), and PolyFit (panel(c)) as well as the ground surveying (blue solid line with x marker).

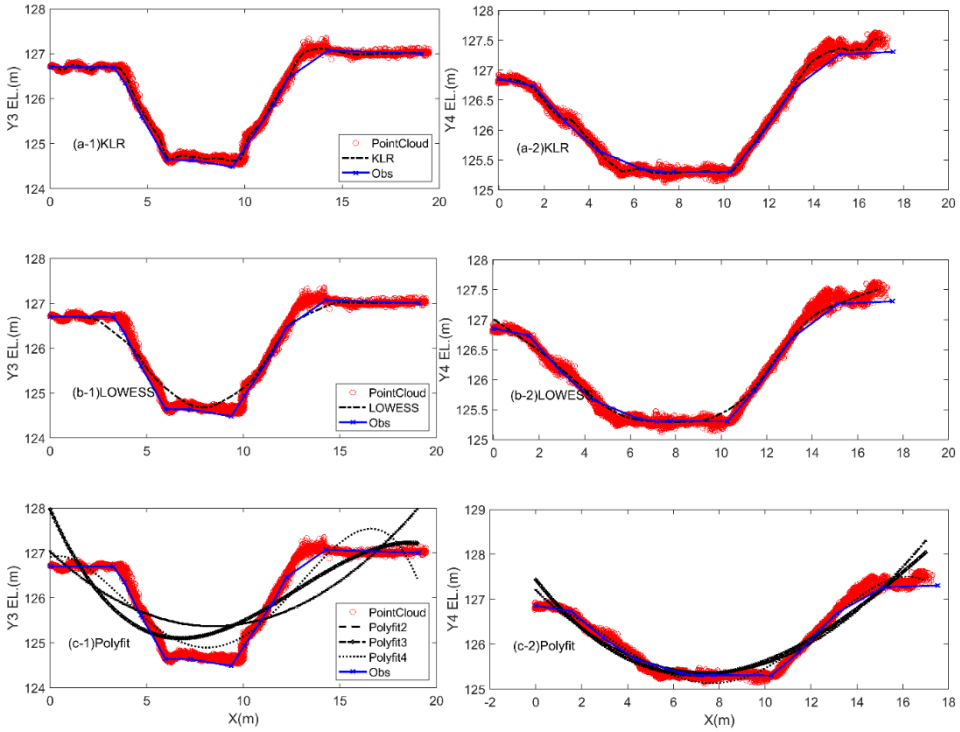

Figure 20. Point cloud data (red circles) for the Y_3 (left panels) and Y_4 (right panels) of Yecheon site and model-fitted line (black dashed line) with KLR (panel(a)), LOWESS (panel(b)), and PolyFit (panel(c)) as well as the ground surveying (blue solid line with x marker).